American Mineralogist, Volume 82, pages 416–422, 1997

Surite: Its Structure and Properties

MOTOKI UEHARA,[1] ATSUSHI YAMAZAKI,[2] AND SADAO TSUTSUMI[1]

[1]Institute of Earth Science, School of Education, Waseda University, 1-6-1 Nishiwaseda, Shinjuku-ku, Tokyo, 169-50 Japan
[2]Department of Mineral Resources Engineering, School of Science and Engineering, Waseda University, 3-4-1 Ohkubo, Shinjuku-ku, Tokyo, 169 Japan

ABSTRACT

Surite has been reported to be a mineral that intercalates cerussite-like materials in a smectite interlayer. However, the chemical analysis and infrared absorption spectra indicate that the interlayer material has the composition of $Ca_{0.5}OH{\cdot}2PbCO_3$. A one-dimensional Fourier synthesis of electron density for acid-treated surite shows that the 2:1 layer of surite has the structure of a general smectite (the distance between the Si plane and the apical O atom plane is about 1.6 Å). Moreover, the one-dimensional Fourier synthesis method showed that the crystal structure of surite is a 2:1 dioctahedral smectite interlayered with basic lead calcium carbonate.

INTRODUCTION

Surite is a naturally occurring clay-inorganic complex, and its only reported occurrence is the Cruz del Sur mine, Argentina. Hayase et al. (1978) reported that the structure of surite is based on a cerussite-like layer intercalated with a 2:1 layer of smectite. However, in their structural model the distance between the Si plane and the apical O atom plane in the tetrahedral sheet is assumed to be 1.97 Å, which is 0.35 Å longer than that in smectites (Fig. 1).

Kampf et al. (1992) described ferrisurite, an Fe^{3+} analog of surite, and suggested that the structure of surite and ferrisurite probably consists of smectite-like layers between which are cerussite-hydrocerussite–like regions of variable composition.

Hayase et al. (1978) assumed that Ca replaces Pb in the interlayer of surite based on the results of wet chemical analysis. However, the cations were distributed so that the entire positive charge in the interlayer became 0.33, based on the composition of cerussite, and an excessive amount of calcium was excluded as an impurity.

In this study, a thin section of surite was reanalyzed by an electron microprobe analyzer (EMPA). The analytical data reveal that most of the Ca is included in the interlayer, which suggests that Ca plays an important role in building the structure of the surite interlayer. On the basis of this observation, the results of recalculation of the crystal structure showed that surite has a 2:1 layer-type structure (Si-O bond distance = 1.62 Å) and its interlayer material is calcium lead carbonate hydroxide, closer in composition to hydrocerussite than to cerussite.

EXPERIMENTAL METHODS

Sample preparation

To determine the 2:1 layer structure of surite, the interlayer materials were removed using the following methods. Surite was treated with 0.36% HCl solution at room temperature for two days and then washed with distilled water. The residue was then dispersed in 1 N $CaCl_2$ solution and stirred using a magnetic stirrer for 24 h. The products were separated centrifugally from the solution, washed five times with distilled water, and then the exchangeable cations in the interlayer were completely exchanged with Ca ions.

Untreated surite and the residue of the acid-treated sample were dispersed in distilled water by ultrasonic vibration. The suspensions were then dropped onto glass slides. These oriented samples were used for XRD measurement for the one-dimensional Fourier synthesis of electron density.

A thin section of surite was prepared for EMPA, and it was also used for X-ray microdiffraction analysis after the conductive carbon coating was removed with ethanol.

Analytical methods

X-ray powder diffraction was performed using a Rigaku Geigerflex RAD-RC diffractometer with graphite-monochromatized Cu$K\alpha$ radiation (55 kV, 200 mA). Synthetic fluorophlogopite mica (Standard Reference Material 675, National Bureau of Standards) was used as the external standard. Each reflection of surite was indexed, and the unit-cell parameters were refined using the program by Appleman and Evans (1973) modified and improved for an NEC PC9801 personal computer. To identify the minerals analyzed with the EMPA, an X-ray microdiffraction procedure was carried out using a Rigaku Micro Diffractometer Ru-200+PSPc/MDGPMA with V-filtered Cr$K\alpha$ radiation (40 kV, 200 mA). Transmission electron microscopy (TEM) was performed on a Philips CM30 at an accelerating voltage of 300 kV.

Chemical analysis was carried out using an energy-dispersive analysis system (Tracor Northern TN5400 EDS

0003–004X/97/0304–0416$05.00

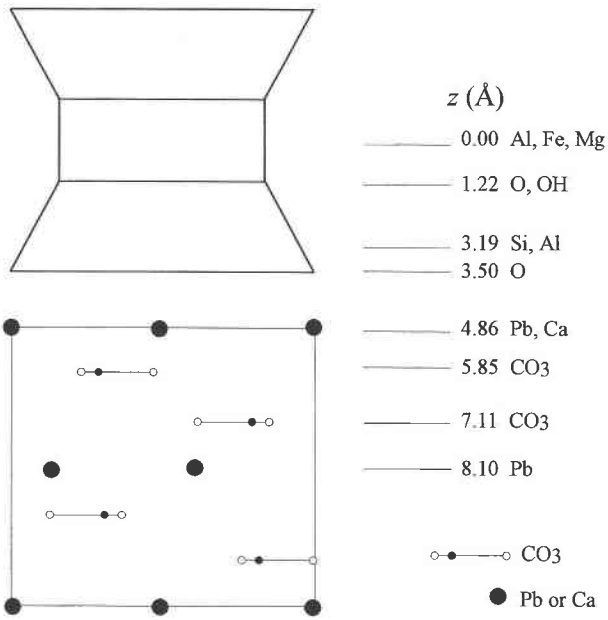

FIGURE 1. The structural model of surite according to Hayase et al. (1978).

unit) installed on an electron microprobe analyzer (JEOL JXA733) using an accelerating voltage of 15 kV and a beam current of 4.00×10^{-10} A. The CO_2 content was determined using a YANACO Type MT-5 CHN CORDER. The H_2O content was obtained by subtracting the CO_2 content from the loss in weight at 1000 °C.

The TG-DTA curves were recorded with a Rigaku Thermoflex TAS-200 at a heating rate of 10 K/min in static air. Evolved gas analysis (EGA) was carried out using a Shimazu TG-GCMS-QP1000EX at a heating rate of 10 K/min in flowing He gas. The IR spectra were recorded with a JASCO FT-IR-8000 spectrometer using the KBr disk method.

RESULTS AND DISCUSSION

Chemical composition and structural formula

The structural formula of surite proposed by Hayase et al. (1978), $(Pb_{1.90}Cu_{0.01}Ca_{0.25})_{2.16}(CO_3)_{2.00}(Al_{1.75}Fe^{3+}_{0.05}Mg_{0.30})_{2.10}(Si_{3.68}Al_{0.32})_{4.00}O_{10}(OH)_2$, did not accurately reflect the chemical analysis that they reported for this mineral, as Kampf et al. (1992) pointed out. This conflict occurred because Hayase et al. (1978) considered the influence of impurities and adjusted the chemical formula to reflect the presence of a cerussite-like material in the interlayer of surite.

Taking into account the interlayer charge of 0.46 obtained from the residue of surite treated with HCl solution in this work, the chemical analytical data of Hayase et al. (1978) were re-calculated and provide the following empirical formula: $(Pb_{1.89}Cu_{0.01}Ca_{0.79}Na_{0.23})_{2.92}(CO_3)_{2.00}(OH)_{1.15}\cdot(Al_{1.72}Fe^{3+}_{0.05}Mg_{0.30})_{2.07}(Si_{3.66}Al_{0.34})_{4.00}O_{10}(OH)_2\cdot 0.35H_2O$.

A thin section of surite was prepared to avoid the influence of the impurities, and measurement of composition of the micro-grains was attempted by EMPA using a highly focused beam (0.1 μm). The CO_2 content was measured with the CHN CORDER. Because this apparatus is capable of analyzing sample sizes <1mg, a very pure sample could be used for analysis. Assuming the interlayer charge to be 0.46, and considering the amounts of H_2O and CO_2 measured by TG and the CHN CORDER, the chemical formula is $(Pb_{1.90}Cu_{0.14}Ca_{0.57})_{2.61}(CO_3)_{1.76}(OH)_{1.24}(Al_{1.77}Fe^{3+}_{0.05}Mg_{0.19})_{2.01}(Si_{3.68}Al_{0.32})_{4.00}O_{10}(OH)_2\cdot 0.49H_2O$, as shown in Table 1. The composition of the interlayer material obtained is very similar to that of the ferrisurite reported by Kampf et al. (1992). In the thin section, five minerals coexisting with surite were confirmed to be chrysocolla, melanotekite, cerussite, quartz, and hematite by both EMPA and X-ray microdiffraction. Even if the beam diameter used for the microprobe analysis were broader, the possibility of additional Ca as an impurity in the measured value is small because these coexisting minerals do not contain Ca as an essential element. As mentioned above, the interlayer material of surite is more sim-

TABLE 1. Chemical composition (wt%) and formula for surite and related samples

	Surite*	Treated surite**	Surite†	Ferrisurite‡
SiO_2	23.95	52.65	23.58	26.6
Al_2O_3	11.55	25.13	11.27	3.2
Fe_2O_3	0.47	0.19	0.41	10.5
MgO	0.85	1.38	1.29	0.2
FeO	—	—	—	0.8
BaO	—	—	—	0.1
CaO	3.46	3.05	4.75	3.4
Na_2O	trace	trace	0.77	0.3
K_2O	trace	trace	—	—
PbO	46.02	trace	45.32	42.7
CuO	1.20	trace	0.07	—
F	—	—	—	0.8
CO_2	8.40	—	9.45	8.2
H_2O^+	3.86	17.60	3.33	3.5
H_2O^-	0.25		0.39	
Total	100.01	100.00	100.63	100.3
Atoms per formula unit containing $O_{10}(OH)_2$				
Si	3.68	3.73	3.66	4.00
[4]Al	0.32	0.27	0.34	0.00
[6]Al	1.77	1.83	1.72	0.57
Fe^{3+}	0.05	0.01	0.05	1.19
Fe^{2+}	—	—	—	0.10
Mg	0.19	0.15	0.30	0.05
Interlayer composition				
Ca	0.57	0.23	0.79	0.55
Na	—	—	0.23	0.09
K	—	—	—	—
Ba	—	—	—	0.01
Pb	1.90	—	1.89	1.73
Cu	0.14	—	0.01	—
CO_3	1.76	—	2.00	1.68
OH	1.24	—	1.15	0.51
F	—	—	—	0.38
H_2O	0.49	3.16	0.35	0.50

* This work.
** The residue obtained from surite pretreated with 0.36% HCl and Ca exchanged.
† Surite, Hayase et al. (1978) recalculated.
‡ Ferrisurite, Kampf et al. (1992).

TABLE 2. XRD data for surite

d_{obs}/Å	d_{calc}/Å	I/I_o*	*hkl*
16.28	16.19	100	001
5.405	5.397	26	003
4.492	4.484	12	020
4.341	4.321	6	021
4.052	4.048	32	004
3.682	3.689	4	014
3.459	3.449	6	023
3.242	3.238	18	005
3.018	3.014	3	$\bar{1}14$
2.865	2.875	7	123
2.700	2.698	11	006
2.590	2.591	10	130
2.314	2.313	9	007
2.245	2.242	4	040
2.163	2.161	3	042
2.064	2.058	4	140
2.024	2.024	2	008
1.962	1.961	3	044
1.845	1.845	2	028
1.798	1.799	1	009
1.696	1.695	4	150
1.617	1.619	1	00,10
1.496	1.495	3	060
1.471	1.472	2	00,11
1.402	1.402	2	064
1.347	1.349	<1	00,12
1.295	1.295	1	256
1.244	1.245	<1	00,13
1.200	1.200	1	11,13
1.156	1.156	1	00,14
1.121	1.121	1	435
1.080	1.079	1	00,15
1.029	1.029	1	$\bar{5}12$
1.012	1.012	1	00,16
0.979	0.979	<1	$\bar{1}90$
0.953	0.952	<1	00,17

* Relative intensities obtained by applying the slit correction.

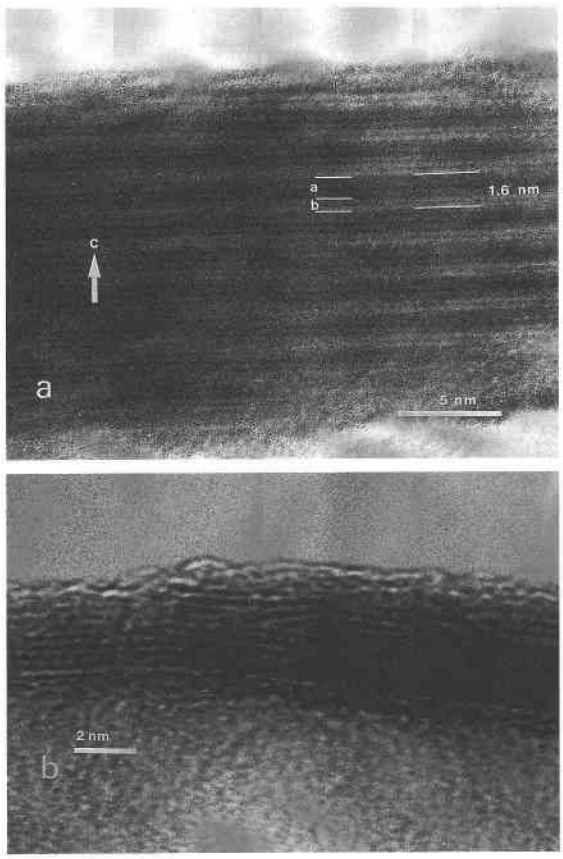

FIGURE 2. (**a**) Lattice image for untreated surite, and (**b**) lattice image for the residue obtained from surite pretreated with 0.36% HCl and Ca-exchanged.

ilar to hydrocerussite than cerussite, as Kampf et al. (1992) pointed out.

A basic lead carbonate-montmorillonite complex, $Pb_{2.90}(CO_3)_{1.82}(OH)_{1.82}(Si_{3.81}Al_{0.19})_{4.00}(Al_{1.70}Fe_{0.15}Mg_{0.15})_{2.00}O_{10}(OH)_2$, intercalated with a hydrocerussite-like layer in the smectite interlayer, has already been synthesized by Tsutsumi et al. (1993). Unlike surite, the hydrocerussite-like layer contains no Ca. Brooker et al. (1983) reported the synthesis of $MOH{\cdot}2PbCO_3$ (M = Na,K) by treatment of hydrocerussite with Na_2CO_3 or K_2CO_3 solutions. The interlayer material of surite, based on the chemical formula, is considered to be Ca-occupied $MOH{\cdot}2PbCO_3$, i.e., $Ca_{0.5}\ OH{\cdot}2PbCO_3$.

XRD and TEM data

Table 2 shows X-ray powder diffraction data for surite. As Kampf et al. (1992) pointed out, a pseudo orthorhombic cell ($\beta = 90°$) is consistent with the X-ray powder diffraction data for surite. The unit-cell parameters obtained were $a = 5.219$ (2), $b = 8.968$ (2), $c = 16.190$ (2) Å, $\beta = 90.13$ (5)° and $V = 757.8$ (6) Å^3. The calculated density of 4.00 g/cm^3 coincides with a measured value of 4.0 g/cm^3 by Hayase et al. (1978), whereas the calculated value from the structural formula proposed by Hayase et al. (1978) is 3.89 g/cm^3.

In the TEM (001) lattice image of untreated surite (Fig. 2a), the contrast between black and white appears to repeat at regular intervals of about 16 Å. It is clear from this image that surite does not display stacking disorder or an interstratified structure. Four sublayers are observed within the 16 Å repeat. It is possible to correlate the layers in the images with different structural layers in surite, at least in a crude way. However, caution is required with this approach, because changes in the image may be related to thickness and focus conditions. In the interlayer space (b in Fig. 2a), the distances between two bright white layers are about 4 Å, and they are probably due to the two Pb layers in the interlayer. In the 2:1 layer space (a in Fig. 2a), the distance between two dark fringes is about 5 Å, and they may be due to the tetrahedral sheet. These observations definitely support our structural model of surite. Figure 2b shows the lattice image of acid-treated surite. This figure shows some stacking faults and no contrast between black and white in the interlayer. Acid treatment caused these differences by decomposing the interlayer material of surite.

Thermal analysis

Figure 3 shows the TG-DTA and EGA curves of surite, which demonstrate that its thermal behavior of surite dif-

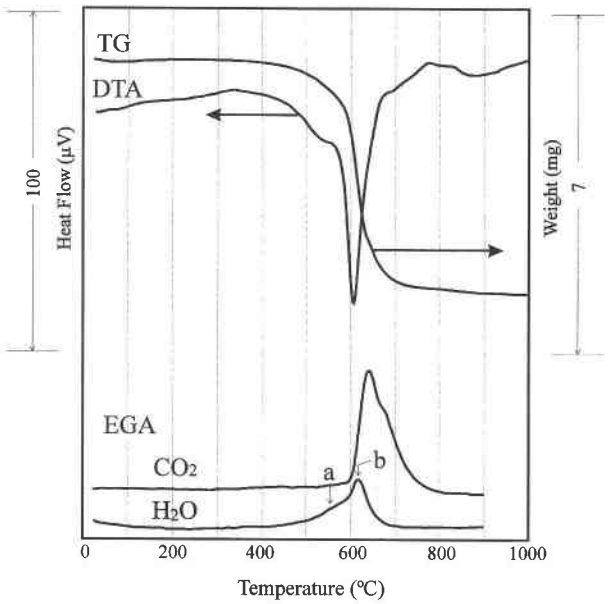

FIGURE 3. TG-DTA and EGA curves of surite. (**a**) H_2O gas evolution due to the dehydroxylation of interlayer material of surite. (**b**) H_2O gas evolution due to the dehydroxylation in the 2:1 layer of surite.

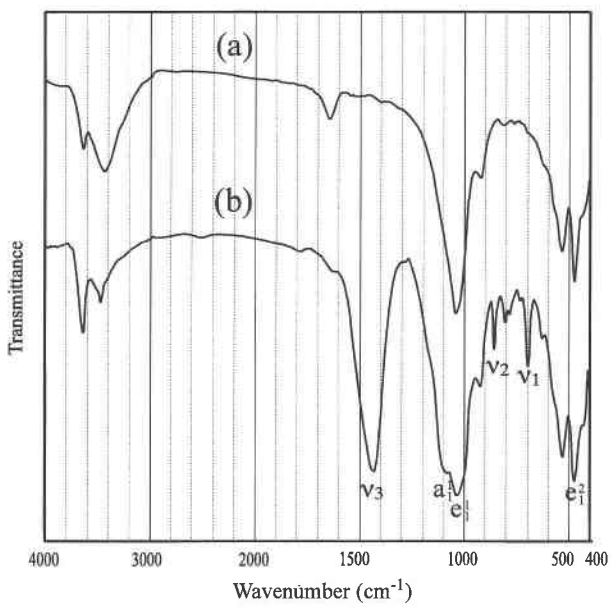

FIGURE 4. Infrared absorption spectra of (**a**) the residue obtained from surite pretreated with 0.36% HCl and Ca-exchanged and (**b**) surite.

fers from that reported by Hayase et al. (1978). Weight loss begins gradually at about 450 °C and occurs rapidly at about 600 °C. An endothermic peak having a shoulder on the low-temperature side, at about 600 °C, is perceptible in the DTA curve. The shoulder with a gradual loss in weight is related to a peak at about 550 °C in the EGA curve.

The EGA curve of H_2O has two peaks (a, b) at 550 and 620 °C. On the basis of the results of the infrared absorption spectra, H_2O gas evolution at 550 and 620 °C is probably due to the dehydroxylation of the interlayer material and the 2:1 layer, respectively. CO_2 gas is generated at a higher temperature than that of dehydroxylation. This suggests that the carbonate component decomposes after the 2:1 silicate layer is dehydrated and destroyed.

Infrared absorption spectra

Figure 4 shows the infrared absorption spectra for surite. Absorption bands at 1424, 853 cm^{-1}, and 693 cm^{-1} are attributed to the carbonate in the interlayer. The absorption band at 918 cm^{-1} is from the bending vibration of Al^{3+}-OH. The absorption band at 527 cm^{-1} is assigned to $^{[6]}$Al-O-$^{[4]}$Si. The absorption bands at 1083, 1034, and 471 cm^{-1} originate in the a^1_1, e^1_1, and e^2_1 vibrations of $(Si_2O_5)_n$, respectively (Kitajima and Takusagawa 1990; Kitajima et al. 1993; Velde 1978). Kitajima et al. (1993) showed that absorption bands at 1085 and 990 cm^{-1} in the IR absorption spectra for fluorine-containing mica are assigned to the a^1_1 and e^1_1 bands from the structural analysis. The a^1_1 and e^1_1 bands correspond to the stretching vibrations of Si-O_a and Si-O_b in the tetrahedral sheet, respectively, where a refers to apical and b to basal. An absorption band around 1000 cm^{-1} for surite is also split into two distinct bands at 1083 and 1034 cm^{-1}, and the intensity ratio is very similar to that reported by Kitajima et al. (1993). For the surite treated with the HCl solution, the absorption band at 1034 cm^{-1} from the vibration of $(Si_2O_5)_n$ did not change in wavenumber; however, no band at 1083 cm^{-1} was discernible. It appears that the Si-O_a bond distance becomes longer and the difference between the Si-O_a and the Si-O_b bond distances becomes smaller following the acid treatment. This change contradicts the structural model of surite proposed by Hayase et al. (1978), which has a long Si-O_a bond distance. Moreover, because the wavenumbers for these absorption bands are almost consistent with those of common smectite, the Si-O bond distance seems to be within the general bond distance of smectite. These observations are consistent with the results obtained by one-dimensional Fourier synthesis in this study.

The absorption band at 3623 cm^{-1} is due to the OH in the 2:1 layer. Kampf et al. (1992) regarded the absorption at 3462 cm^{-1} as resulting from H_2O similar to that in smectite. Little interlayer H_2O exists in surite judging from the small weight loss below 200 °C in the TG data, although absorption that is certainly due to the presence of interlayer H_2O appears at approximately 3460 cm^{-1} in smectite. Moreover, the pattern of this absorption is very sharp compared with that due to the interlayer water of smectite. The infrared absorption spectra of surite and the residue after the HCl treatment over the region of 3000 cm^{-1}–4000 cm^{-1} are also shown in Figure 5. The pattern and wave number of absorption from the interlayer H_2O of the residue differ from those of surite. These obser-

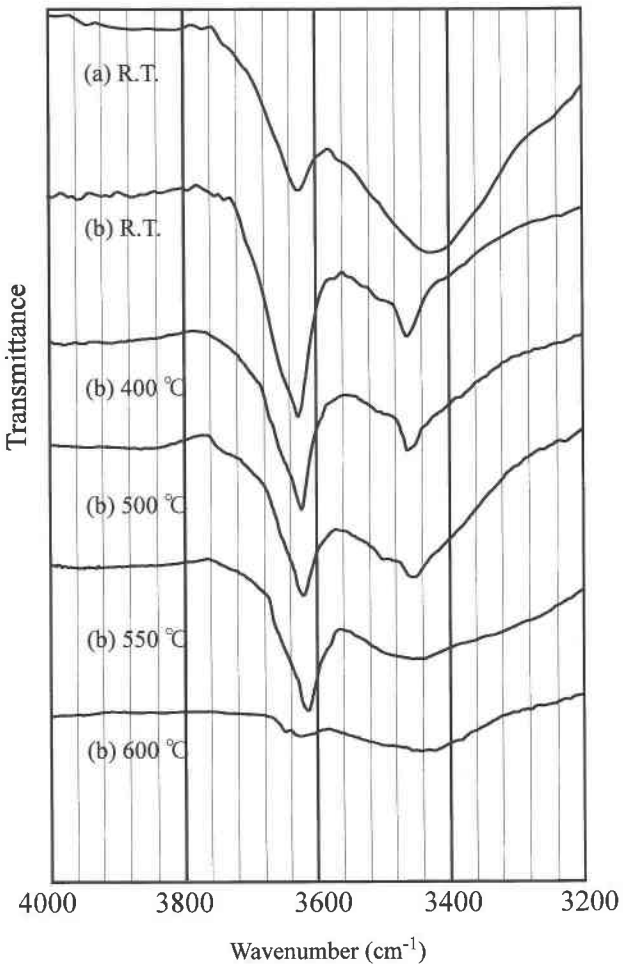

FIGURE 5. Infrared absorption spectra of (**a**) the residue obtained from surite pretreated with 0.36% HCl and Ca-exchanged and (**b**) surite at various temperatures.

vations support the belief that surite has OH in the interlayer sites.

The absorption caused by OH in the interlayer becomes broad at 500 °C and is not discernible at 550 °C. The absorption from OH in the 2:1 layer is maintained up to 550 °C but is not discernible at 600 °C. This observation indicates that dehydroxylation of the interlayer material occurs before that of the 2:1 layer, and two peaks in the EGA curves of H_2O (Fig. 3) correspond to the respective dehydroxylation events of these two distinct types of H_2O in the surite structure.

STRUCTURAL FORMULA AND STRUCTURAL MODEL

In the structural model of surite (Hayase et al. 1978), the distance between the Si plane and the apical O atom plane is 1.97 Å, 20% longer than the 1.6[2] Å of the typical Si-O bond distance. To clarify the structure of the 2:1 layer of surite, the acid-treated sample that was subsequently Ca-saturated, was examined by one-dimensional electron density analysis. Stacking disorder in the acid-

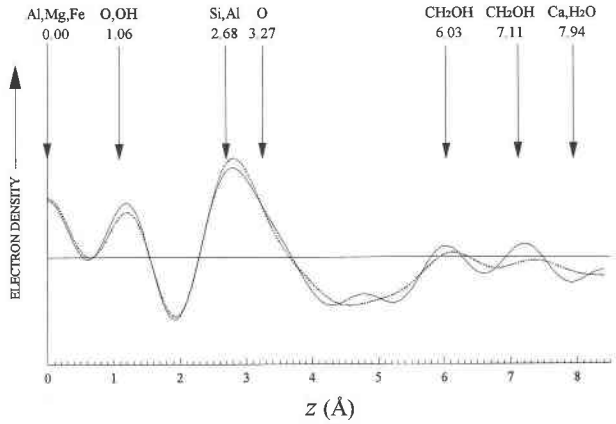

FIGURE 6. One-dimensional curves of electron density as a function of z values from 00l diffraction intensities of the residue obtained from surite pretreated with 0.36% HCl and Ca-exchanged, treated with ethylene glycol. Solid line: calculated. Dotted line: observed.

treated surite disturbs the high-order reflections, making the analysis difficult. Hence, a sample treated with ethylene glycol was examined. The atomic coordinates of the ethylene glycol, the Ca cation, and the H_2O in the interlayer were taken from the model by Reynolds (1965). When the one-dimensional electron density is calculated on the basis of the atomic coordinates of the 2:1 layer structure model by Hayase et al. (1978), the calculated electron density distribution does not agree with the observed distribution and the reliability factor is 0.6. When the atomic coordinates of ordinary smectite (Si-O distance = 1.62 Å) are used for the 2:1 layer, the reliability factor improves to a value of 0.12 and a refined result is obtained. Figure 6 shows the observed and calculated one-dimensional electron density distribution curves obtained by the Fourier synthesis method, and the refined structural model is also shown with atomic parameters.

TABLE 3. Observed and calculated structural factors of 00l reflections for the residue obtained from surite pretreated with 0.36% HCl and Ca exchanged

00l	d_{00l} (Å)	I/I_0	$\lvert F_{obs}\rvert$	F_{calc}*
1	16.79	100	76.64	74.28
2	8.402	3.667	29.39	32.95
3	5.597	4.845	50.95	−46.45
4	4.203	0.763	27.18	−29.59
5	3.358	6.316	98.85	98.71
6	2.798	2.317	72.79	60.29
7	2.400	0.091	17.07	−17.00
8	2.100	0.747	56.94	−66.68
9	1.868	0.410	48.34	−47.86
10	1.679	0.064	21.63	−22.05
11	1.527	0.192	41.83	41.45
12	1.401	0.221	49.56	49.62
13	1.291	0.150	44.49	28.35
14	1.200	0.053	28.42	55.95
15	1.119	0.018	17.33	17.58
16	1.050	0.010	13.66	14.34

* Obtained from the final z parameters (Fig. 6). R = 0.12.

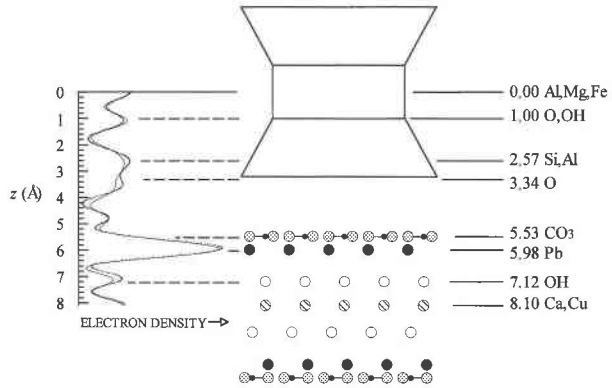

FIGURE 7. One-dimensional curves of electron density as a function of z values from 00l diffraction intensities of surite. Solid line: calculated. Dotted line: observed. The corresponding structural model is shown.

TABLE 4. Observed and calculated structural factors of 00l reflections for surite

00l	d_{00l} (Å)	I/I_0	$\|F_{obs}\|$	F_{calc}*
1	16.28	100	35.35	−28.85
2			0.00	−6.94
3	5.405	25.600	54.49	61.77
4	4.052	31.514	81.45	−79.77
5	3.242	18.320	78.59	61.87
6	2.700	7.339	60.62	56.32
7	2.314	10.260	85.05	−87.41
8	2.024	1.536	38.32	47.07
9	1.798	0.510	25.34	−31.05
10	1.617	0.789	35.68	−36.06
11	1.471	1.511	55.14	55.06
12	1.347	0.374	30.29	−30.22
13	1.244	0.214	24.87	24.87
14	1.156	1.457	69.15	56.45
15	1.080	0.733	51.13	−39.19
16	1.012	0.249	30.29	38.84

* Obtained from the final z parameters (Fig. 7). R = 0.12.

Table 3 shows the comparison of the calculated and observed structural factors of the 00l reflections.

The structure of surite was re-examined by the one-dimensional Fourier synthesis method of electron density on the basis of the following results: (1) The one-dimensional Fourier synthesis method clarified that natural surite with the interlayer materials removed by HCl treatment has the crystal structure of smectite. (2) The chemical composition suggests that the interlayer material is $Ca_{0.5}OH{\cdot}2PbCO_3$ rather than $PbCO_3$. (3) The absorption from OH in the interlayer is observed in the infrared absorption spectra. (4) OH in the interlayer seems to exist in ferrisurite, in which the interlayer material is similar in composition to $Ca_{0.5}OH{\cdot}2PbCO_3$ (Kampf et al. 1992). As a result, the structure of the carbonate in the surite interlayer is regarded as being based on $Ca_{0.5}OH{\cdot}2PbCO_3$, similar to the hydrocerussite structure.

The crystal structure of $Ca_{0.5}OH{\cdot}2PbCO_3$ has not been reported, but the cell parameters for $MOH{\cdot}2PbCO_3$ (M = K or Na) have been indexed on the basis of a hexagonal unit cell, with a = 5.3473, c = 13.990 Å (K) and a = 5.2727, c = 13.447 Å (Na) (Brooker et al. 1983). The cell parameters for hydrocerussite were indexed on the basis of a hexagonal unit cell, with a = 5.2400, and c = 23.681 Å (Korokoros and Vassiliadis 1953). The thickness of each molecular layer is 6.995, 6.7235, and 7.913 Å for K, Na, and hydrocerussite, respectively. The basal spacing of surite, 16.2 Å, is 1.2 Å smaller than the 17.4 Å value for a basic lead carbonate-montmorillonite complex (Tsutsumi et al. 1993). On the basis of the thickness of the interlayer, it is reasonable to assume that a molecular layer material, represented as $MOH{\cdot}2PbCO_3$, intercalates into the surite interlayer. Figure 7 shows the best fit between the observed and calculated one-dimensional electron density distribution curves that were obtained by the Fourier synthesis method. The refined structural model of surite is also shown with atomic parameters. Table 4 shows the comparison of the calculated and observed structural factors of the 00l reflections. The reliability factor, obtained using reflections up to the sixteenth order, is 0.12; therefore, the structural model appears reasonable, although a reliability factor of 0.26 was obtained by using up to the ninth order reflection by Hayase et al. (1978). The interlayer cation planes occur at two levels in Figure 7. One is located in the middle of the calcium lead carbonate hydroxide layer (z = 8.1 Å), and the other is between the CO_3 and OH planes (z = 5.98 Å). The distribution of the cation between the inner and outer cation planes is $Pb^*_{1.90}(Ca_{0.57}Cu_{0.14})_{0.71}(CO_3)_{1.76}(OH)_{1.24}$, where Pb* is defined as the cation of the outer plane. Because the cation distribution of $MOH{\cdot}2PbCO_3$ is represented as $MOH{\cdot}2Pb^*CO_3$, the result by one-dimensional electron density analysis is consistent with the distribution of cations for this structural formula. Therefore, the surite interlayer has the structure of a calcium hydroxide layer, $Ca(OH)_2$, sandwiched between lead carbonate layers, $PbCO_3$.

ACKNOWLEDGMENTS

We are indebted to Dr. M. Shiraishi, National Research Institute for Resource and Environment, for permission to use the Institute's CM30 transmission electron microscope. This study was partially supported by a Waseda University Grant for Special Research Projects (94B-37).

REFERENCES CITED

Appleman, D.E., and Evans, H.T. Jr. (1973) Job 9214: Indexing and Least-squares Refinement of Powder Diffraction Data. U.S. Geological Survey, Computer Contribution 20, U.S. National Technical Information Service. Document PB-16188.

Brooker, M.H., Sunder, S., Taylor, P., and Lopata, V.J. (1983) Infrared and Raman spectra and X-ray diffraction studies of solid lead (II) carbonates. Canadian Journal of Chemistry, 61, 494–502.

Hayase, K., Dristas, J.A., Tsutsumi, S., Otsuka, R., Tanabe, S., Sudo, T., and Nishiyama, T. (1978) Surite, a new Pb-rich layer silicate mineral. American Mineralogist, 63, 1175–1181.

Kampf, A.R., Jackson, L.L., Sidder, G.B., Foord, E.E. and Adams, P.M. (1992) Ferrisurite, the Fe^{3+} analogue of surite, from Inyo County, California. American Mineralogist, 77, 1107–1111.

Kitajima, K., Fujita, T., Utsumi, K., Taruta, S., and Takusagawa, N. (1993) Effects of heat treatment on IR spectra and b-axis values of cation-exchanged fluorine micas. Nippon Kagaku Kaishi, 6, 778–781.

Kitajima, K., and Takusagawa, N. (1990) Effects of tetrahedral isomorphic substitution on the IR spectra of synthetic fluorine micas. Clay Minerals, 25, 235–241.

Korokoros, P. and Vassiliadis, K. (1953) Röntgenkristallographie von Hydrocerussit. Tschermaks Minerlogische und Petrographische. Mitteilungen, 3, 298–304.

Reynolds, R.C. (1965) X-ray study of an ethylene glycol-montmorillonite complex. American Mineralogist, 50, 990–1001.

Tsutsumi, S., Yamazaki, A., Uehara, M., and Otsuka, R. (1993) Preparation and properties of a basic lead carbonate-montmorillonite complex. Clay Minerals, 28, 13–24.

Velde, B. (1978) Infrared spectra of synthetic micas in the series muscovite-MgAl celadonite. American Mineralogist, 63, 343–349.

Manuscript received April 5, 1996
Manuscript accepted December 6, 1996